Journal of Applied Polymer Science

Fabrication of thermoresponsive, core-crosslinked micelles based on poly[*N*-isopropyl acrylamide-*co*-3-(trimethoxysilyl)propylmethacrylate]-*b*-poly{*N*-[3-(dimethylamino)propyl]methacrylamide} for the codelivery of doxorubicin and nucleic acid

Cong Chang,[1] Hong Dan,[1] Li-Ping Zhang,[1] Ming-Xiang Chang,[2] Yin-Feng Sheng,[2] Guo-Hua Zheng,[1] Xian-Zheng Zhang[3]

[1]Key Laboratory of Chinese Medicine Resource and Compound Prescription of Ministry of Education, Hubei University of Chinese Medicine, Wuhan 430065, People's Republic of China

[2]Affiliated Hospital, Hubei University of Chinese Medicine, Wuhan 430061, People's Republic of China

[3]Key Laboratory of Biomedical Polymers of Ministry of Education and Department of Chemistry, Wuhan University, Wuhan 430072, People's Republic of China

Correspondence to: G.-H. Zheng (E-mail: 1080697@qq.com) and X.-Z. Zhang (E-mail: xz-zhang@whu.edu.cn)

ABSTRACT: Thermoresponsive amphiphilic copolymer, poly[*N*-isopropyl acrylamide-*co*-3-(trimethoxysilyl)propylmethacrylate]-*b*-poly{*N*-[3-(dimethylamino)propyl]methacrylamide} with a branched structure was designed and synthesized by consecutive reversible addition–fragmentation chain-transfer polymerization. The further hydrolysis of trimethoxysilyl functions in 3-(trimethoxysilyl) propyl methacrylate units led to the fabrication of core-crosslinked (CCL) micelles with silica crosslinks at temperatures above the lower critical solution temperature of the poly(*N*-isopropyl acrylamide) block. The thermally induced structural and morphological changes of the CCL micelles in aqueous solution were investigated by transmission electron microscopy and ^{1}H-NMR analyses. The resulting CCL micelles were further explored as nanocarriers for the codelivery of an anticancer drug and nucleic acid for enhanced therapeutic efficacy. The CCL micelles effectively condensed the nucleic acid and mediated higher gene transfer in the presence of serum than in serum-free transduction. A cytotoxicity study revealed that whereas the pure CCL micelles exhibited unapparent cytotoxicity, the codelivery of p53 and doxorubicin with the CCL micelle formulation resulted in better treatment efficiency than sole chemotherapy. © 2014 Wiley Periodicals, Inc. J. Appl. Polym. Sci. **2015**, *132*, 41752.

KEYWORDS: biomaterials; crosslinking; drug-delivery systems; micelles; stimuli-sensitive polymers

Received 18 August 2014; accepted 3 November 2014
DOI: 10.1002/app.41752

INTRODUCTION

During the past several decades, core–shell micelles self-assembled from amphiphilic copolymers have attracted broad attention because of their great potential for applications in biomedicine as nanosized carriers for drug and gene delivery.[1–3] Chemotherapy has been used extensively to treat various cancers; however, its clinical application has been significantly hampered by the low aqueous solubility and bioavailability of anticancer drugs, multidrug resistance, drug-associated side effects, and so on.[4–6] To conquer these deficiencies of pure chemotherapy, the codelivery of drug and plasmid DNA has emerged as an exciting therapeutic strategy for its synergistic effect, which offers advantages in these aspects, including reduced drug resistance, enhanced antitumor activity, and decreased drug dosage and toxicity.[7,8] Wang *et al.*[9] developed cationic core–shell nanoparticles self-assembled from poly{(*N*-methyldietheneamine sebacate)-*co*-[(cholesteryl oxocarbonylamido ethyl) methyl bis(ethylene) ammonium bromide] sebacate}. Cancer growth was suppressed by the codelivery of paclitaxel with an interleukin-12-encoded plasmid more efficiently than by the simple delivery of either paclitaxel or the plasmid DNA (pDNA). Shi *et al.*[10] synthesized a series of amphiphilic triblock copolymers based on monomethoxy poly(ethylene glycol) (mPEG)–poly(ε-caprolactone)–polyethylenimine and investigated their application for the codelivery of the chemotherapeutic drug doxorubicin (DOX) and pDNA simultaneously. These studies demonstrated that cationic micelle carriers could encapsulate the drug and condense the pDNA efficiently, increase the cellular uptake *in vitro*, and achieve a high gene transfection efficiency. These findings have inspired the rapid

development of cationic polymeric micelles consisting of a cationic shell for pDNA condensation and a hydrophobic core for lipophilic drug encapsulation in recent years.[11,12]

Another important consideration in the clinical translation of drug and gene carriers is the controlled synthesis of well-defined materials.[13,14] Among all of the controlled living radical polymerization techniques, reversible addition–fragmentation chain transfer (RAFT) polymerization seems the most powerful synthetic tool in the preparation of various well-defined (co)polymers with diverse functionalities. It can be accomplished under very mild reaction conditions and provides access to the widest range of monomers.[15–17] Recently, RAFT polymerization has been reported to synthesize several branched polymers by the use of AB_2 macromonomers,[18] divinyl monomers,[19] and crosslinking agents.[20] Notably, Vogt and Sumerlin[21] simultaneously prepared a temperature-responsive branched poly(*N*-isopropyl acrylamide) (PNIPAAm) via a compound containing a reversible chain-transfer function and a vinyl group by RAFT polymerization. Thurecht *et al.*[22] synthesized hyperbranched polymers using ethylene glycol dimethacrylate as a branching agent by the RAFT technique.

Relative to linear polymers, branched polymers displayed unique properties, such as a high solubility, low viscosity, and large amount of modifiable peripheral groups, on the surface because of their decreased chain entanglement, reduced hydrodynamic volume, highly branch three-dimensional globular structure, and so on.[23,24] Cationic branched polymers could easily self-assemble with and condense pDNA to form stable nanoparticles by electrostatic interactions compared to virus and liposome gene carriers; meanwhile, they offer advantages over virus vectors, such as safety, low immunogenicity, low cost, and easy industrialization. Therefore, the design and synthesis of cationic polymers as efficient gene vectors have been hot subjects of research.[25,26] Wang *et al.*[27] synthesized a series of cationic poly(amido amine)s (PAAs) with different branched architectures. Their study showed that the increased branches of PAAs led to a better buffering capacity, stronger DNA condensation, and lower cytotoxicity. In another example, the new hyperbranched PAAs with disulfide linkages reported by Martello *et al.*[28] mediated a higher gene transfection efficiency than their linear counterparts.

In this study, the anticancer drug DOX and plasmid53 (p53) were chosen as the therapeutics on the basis of the following considerations. DOX is frequently used in chemotherapy; it can damage pDNA by intercalating with the base pairs of pDNA and inhibiting nucleic acid replication.[29,30] Further, it kills cancer cells mainly by apoptosis.[31] The p53 tumor suppressor gene is a transcriptional regulator that can inhibit cell proliferation through apoptosis and/or G1-cell cycle arrest in mammalian cells.[32] Notably, the transcription of p53 promotes the sensitivity of tumor cells to DOX and results in tumor growth inhibition and prolonged survival in murine models.[33,34] In our design, the cationic *N*-[3-(dimethylamino)propyl]methacrylamide (DMAPMAm) block was easy to prepare with its readily engineered structure and molecular weight for pDNA condensation.[35] The other temperature-sensitive block based on *N*-isopropyl acrylamide (NIPAAm) and 3-(trimethoxysilyl) propyl methacrylate (MPMA) was included to provide structural stability for the poly{*N*-[3-(dimethylamino)propyl]methacrylamide} (PDMAPMAm)/pDNA complex and to generate a hydrophobic core for DOX encapsulation by sol–gel-catalyzed self-crosslinking in an aqueous medium.[36] Such an amphiphilic copolymer poly[*N*-isopropyl acrylamide-*co*-3-(trimethoxysilyl)propylmethacrylate] [P(NIPAAm-*co*-MPMA)]-*b*-PDMAPMAm with a branched structure was synthesized by successive RAFT polymerization. Core-crosslinked (CCL) micelles were further fabricated by a two-step approach, that is, the self-assembly of the amphiphilic copolymer in an aqueous phase at the temperature above the lower critical solution temperature (LCST) of PNIPAAm followed by the crosslinking of the micellar core with an inorganic silica-based crosslinking strategy. The DOX and plasmid were further loaded into and condensed with the CCL micelles via hydrophobic and electrostatic interactions, respectively. The *in vitro* cytotoxicity of the pure CCL micelles, DOX-loaded CCL micelles, and DOX- and p53-loaded CCL micelles were investigated to evaluate their efficiency for tumor therapy.

EXPERIMENTAL

Materials

NIPAAm (Acros), MPMA (Wuhan University Chemical Plant, Wuhan, China), and 2-aminoethyl methacrylate (Sigma) were used as received. DMAPMAm was purchased from Sigma-Aldrich. *N,N′*-Dimethylformamide (DMF), tetrahydrofuran (THF), *N*-methyl pyrrolidone, ethyl acetate, and triethylamine (TEA) were obtained from Shanghai Chemical Reagent Co. and were used after distillation. *N,N′*-Dicyclohexylcarbodiimide and 4-dimethylamiopryidine were obtained from Shanghai Chemical Reagent Co. (China). 2-(2-Carboxyethylsulfanylthiocarbonylsulfanyl) propionic acid (CPA) and 2-(phenylcarbonothioylthio) acetic acid (PAA) were prepared according to previous publications.[1,17] *N,N′*-Azobisisobutyronitrile (AIBN) was purchased from Shanghai Chemical Reagent Co. and was used after recrystallization. Doxorubicin hydrochloride was purchased from Zhejiang Hisun Pharmaceutical Co., Ltd. (China) and was used as received. Dialysis tubes (molecular weight cutoff = 8000–12,000 g/mol) and pore-sized syringe filters (0.45 μm) were purchased from Shanghai Chemical Reagent Co. All of the other reagents and solvents were used without further purification.

Synthesis of 2-[2-(Phenylcarbonothioylthio)acetamido]ethyl Methacrylate (PAEM). PAA (848 mg, 4 mmol), *N,N′*-dicyclohexylcarbodiimide (824 mg, 4 mmol), and 4-dimethylamiopryidine (586 mg, 4.8 mmol) were dissolved in 30 mL of anhydrous THF in a 150-mL, round-bottomed flask equipped with a magnetic stirring bar. The mixture was stirred for 4 h and then filtered. The resulting brownish red solution was poured into the *N*-methyl pyrrolidone solution, which dissolved 2-aminoethyl methacrylate (830 mg, 5 mmol) and TEA

(505 mg, 5 mmol) and was stirred overnight at room temperature. After the reaction, the mixed solution was filtered again and concentrated under reduced pressure. The concentrated solution was added dropwise into distilled water, and the resulting brownish red oily precipitate was collected by centrifugation. Finally, the PAEM was purified by extraction with dichloromethane from distilled water three times and then dried *in vacuo*.

^{1}H-NMR ($CDCl_3$, 300 Hz, δ, ppm): 1.93 (3H, CH_3—C═), 3.48 (2H, —NH—CH_2—), 3.72 (2H, —S—CH_2—), 4.56 (2H, —CH_2—O—), 5.66 (1H, ═CH_2), 6.19 (1H, ═CH_2), 7.58 (2H, Ar—H), 7.78 (1H, Ar—H), 8.02 (2H, Ar—H).

Synthesis of P(NIPAAm-*co*-MPMA) (macro-CTA) by RAFT Polymerization. NIPAAm (2.28 g, 20 mmol), MPMA (95.3 μL, 0.4 mmol), CPA (25.4 mg, 0.1 mmol), and AIBN (1.64 mg, 0.01 mmol) were dissolved in anhydrous THF (15 mL, freshly distilled) in a thoroughly dried glass flask equipped with a magnetic stirring bar. The reaction mixture was degassed and then sealed. The flask was immersed in an oil bath preheated to 70°C to start the polymerization. After 70 min of polymerization, the reaction flask was removed from the oil bath. Then, the reaction mixture was poured into diethyl ether to precipitate the product. The product was collected by filtration, purified twice by redissolution/reprecipitation with THF/diethyl ether, and finally dried *in vacuo* overnight to obtain macro chain transfer agent (macro-CTA).

Synthesis of Branched P(NIPAAm-*co*-MPMA)-*b*-PDMAPMAm by RAFT Polymerization. DMAPMAm (800 mg, 4.7 mmol), PAEM (28.8 mg, 0.08 mmol), macro-CTA (200 mg, 0.014 mmol), and AIBN (1 mg, 0.006 mmol) were dissolved in anhydrous THF (15 mL, freshly distilled) in a dried glass flask equipped with a magnetic stirring bar. The reaction mixture was degassed and then sealed. Then, the flask was immersed in an oil bath preheated to 70°C. After polymerization for 25 h, the reaction flask was removed from the oil bath, and the reaction mixture was poured into cold diethyl ether to precipitate the resulting copolymer. The product was collected by filtration, purified twice by redissolution/reprecipitation with THF/diethyl ether, and finally dried *in vacuo* overnight.

^{1}H-NMR Characterization

^{1}H-NMR spectra were recorded on a Varian Unity 300-MHz spectrometer with $CDCl_3$ and D_2O as the solvents, respectively. The testing temperature was set at 20°C without specific explanation.

Size-Exclusion Chromatography (SEC)–Multiangle Laser Light Scattering (MALLS) Measurements

SEC–MALLS analysis was used to determine the molecular weights of the polymers. A dual-detector system consisting of a MALLS device (DAWN EOS, Wyatt Technology) and an interferometric refractometer (Optilab DSP, Wyatt Technology) was used. The columns used were Styragel HR1 and HR4. The concentration of the copolymer was kept constant at 10 mg/mL, and THF (chromatographic grade) was used as the eluent at a flow rate of 0.3 mL/min. The MALLS detector was operated at a laser wavelength of 690 nm.

Micelle Formation

The CCL micelle was prepared by the direct dissolution of 3 mg of the branched P(NIPAAm-*co*-MPMA)-*b*-PDMAPMAm copolymer in 0.5 mL of distilled water at 20°C; this solution was then added dropwise into 9.5 mL of distilled water thermostated at 45°C under vigorous stirring. After the sol–gel process (15 h), the mixture solution was transferred into a dialysis tube and dialyzed against distilled water to remove methanol from the hydrolysis of the silyl ethers.

Transmission Electron Microscopy (TEM) Observation

A drop of micelle suspension was placed on a copper grid with carbon film and stained by a 0.2% w/v solution of phosphotungstic acid before observation by a JEM-100CX II TEM instrument at an acceleration voltage of 100 keV.

Size Distribution Measurement

A Zetasizer Nano ZS (Malvern Instruments) was used to determine the size and size distribution of the crosslinked micelles. The micelle solution (500 mg/L) was passed through a 0.45-μm pore size filter before the measurements.

LCST Behaviors

The optical absorbance of the CCL-branched P(NIPAAm-*co*-MPMA)-*b*-PDMAPMAm micelle solution (300 mg/L) at various temperatures was measured at 500 nm with a Lambda Bio40 ultraviolet–visible spectrometer (PerkinElmer). Sample cells were thermostated in a circulator bath at different temperatures from 25 to 53°C before the measurements, and the heating rate was set at 0.1°C/min. The LCST was defined as the temperature that produced half of the total increase in optical absorbance.

Drug Loading (DL) and *In Vitro* Drug Release

DOX HCl (0.6 mg) was stirred with 300 μL of TEA in 1.0 mL of DMF overnight to obtain the DOX. Then, the branched P(NIPAAm-*co*-MPMA)-*b*-PDMAPMAm copolymer (6 mg) was dissolved in the solution. The solution was added to 20 mL of distilled water at 40°C under stirring to form drug-loaded CCL micelles. After the sol–gel process, the CCL micelle solution was put into a dialysis tube and subjected to dialysis against 1 L of distilled water at 40°C for 24 h. The distilled water was renewed every 8 h to remove the unloaded free drug and DMF. The solution was equipartitioned into two parts, and each was placed into a dialysis tube. Then, we immersed the tube into phosphate buffer saline (PBS) (pH 7.4, $I = 0.1$, where I is ionic strength) at 20 and 40°C, respectively.

The volume of PBS for drug-release study was 10 mL, which was withdrawn periodically and held constant by adding 10 mL of fresh medium after each sampling. The total amount of DOX loaded in the micelles was calculated as the summation of cumulative amount of drug released from the micelles and the amount of drug remaining in the micelles after release. The amount of DOX released from micelles was measured with UV absorbance at 232 nm.[37,38] To determine the amount of drug retained in the micelles, the micelle suspension after drug release was freeze-dried and then dissolved in DMF and analyzed by UV absorbance at 497 nm. The entrapment efficiency (EE) and DL capacity were calculated on the basis of the following formulas:

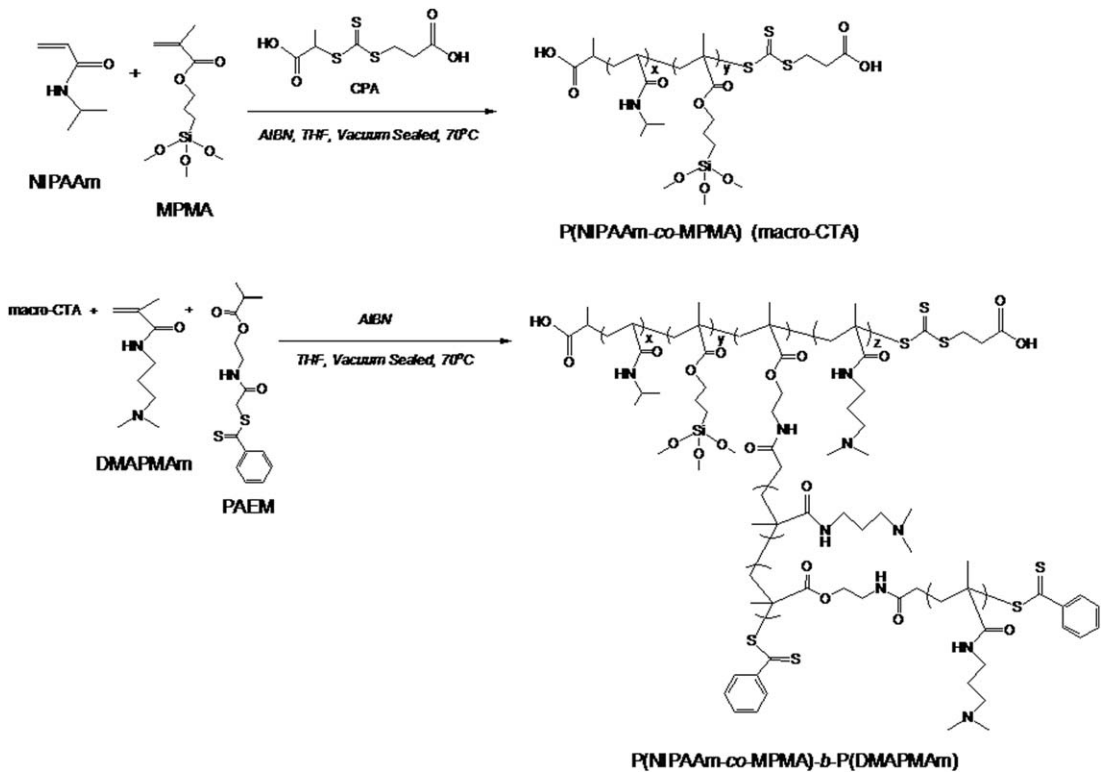

Scheme 1. Synthesis of the branched P(NIPAAm$_{188}$-*co*-MPMA$_4$)-*b*-P(DMAPMAm$_{92}$) copolymers.

EE=(Mass of drug loaded in the micelles/ Mass of drug fed initially)×100%,

DL=(Mass of drug loaded in the micelles/ Mass of drug−loaded micelles)×100%.

Agarose Gel Retardation Assay

A series of CCL micelle/DNA complexes at different weight ratios were prepared by the addition of an appropriate volume of CCL micelles (in 150 m*M* NaCl solution) to 0.5 μL of plasmid pGL-3 DNA (200 ng/μL in 40m*M* Tris-HCl buffer solution). The complexes were diluted by a 150 m*M* NaCl solution to 8 μL, and then, the complexes were incubated at 37°C for 30 min. Thereafter, the complexes were electrophoresed on a 0.7% w/v agarose gel containing GelRed with Tris-acetate running buffer at 80 V for 60 min. The DNA was visualized with a UV lamp with a Vilber Lourmat imaging system (France).

In Vitro Transfection Study

For the transfection studies, 293T cells were seeded at a density of 6 × 10^4 cells/well in 24-well plate with 1 mL of Dulbecco's modified Eagle medium (DMEM) containing 10% fetal calf serum (FBS); they were then incubated at 37°C for 24 h before the addition of the CCL micelle/pDNA complexes. After the cells were washed with PBS, the CCL micelle/pGL-3 complexes were added with serum-free DMEM or serum-containing DMEM, respectively, and subjected to further incubation for 4 h at 37°C. Next, the serum-free DMEM or serum-containing DMEM was replaced by fresh culture media, and the cells were incubated for another 44 h. Finally, the medium was removed, and the cells were washed with PBS. Then, the cells were lysed with 200 μL of reporter lysis buffer (Pierce), The luciferase activity was measured with a chemiluminometer (Lumat LB9507, EG&G Berthold, Germany). The empirical procedure of the transfection studies in the HeLa cells was the same as mentioned previously (where HeLa cell is one of cervical cancer cell).

In Vitro Antitumor Efficacy of DOX- and p53-Loaded CCL Micelles

The cytotoxicities of the CCL micelles, DOX-loaded CCL micelles, and DOX- and p53-loaded CCL micelles were examined by 3-(4,5-dimethyl-2-thiazolyl)-2,5-diphenyl-2-H-tetrazolium bromide (MTT) assay. Briefly, the HeLa cells (6000 cells/well) were seeded in a 96-well plate with 100 μL of DMEM containing 10% FBS. After incubation for 24 h (37°C, 5% CO_2), the culture medium was removed, and DMEM with different concentrations of CCL micelles, DOX-loaded CCL micelles, and DOX- and p53-loaded CCL micelles were added to each well, respectively. After incubation at 37°C for 4 h, the DMEM medium with micelles was replaced with 1 mL of fresh DMEM, and the cells were further incubated at 37°C for 24 h. Finally, 20 μL of MTT solution (5 mg/mL) was added to each well. After incubation for 4 h, the MTT medium was removed from each well, and 150 μL of dimethyl sulfoxide was added. The absorbance was measured at 570 nm with a microplate reader (Bio-Rad, model 550). The relative cell viability was calculated as follows:

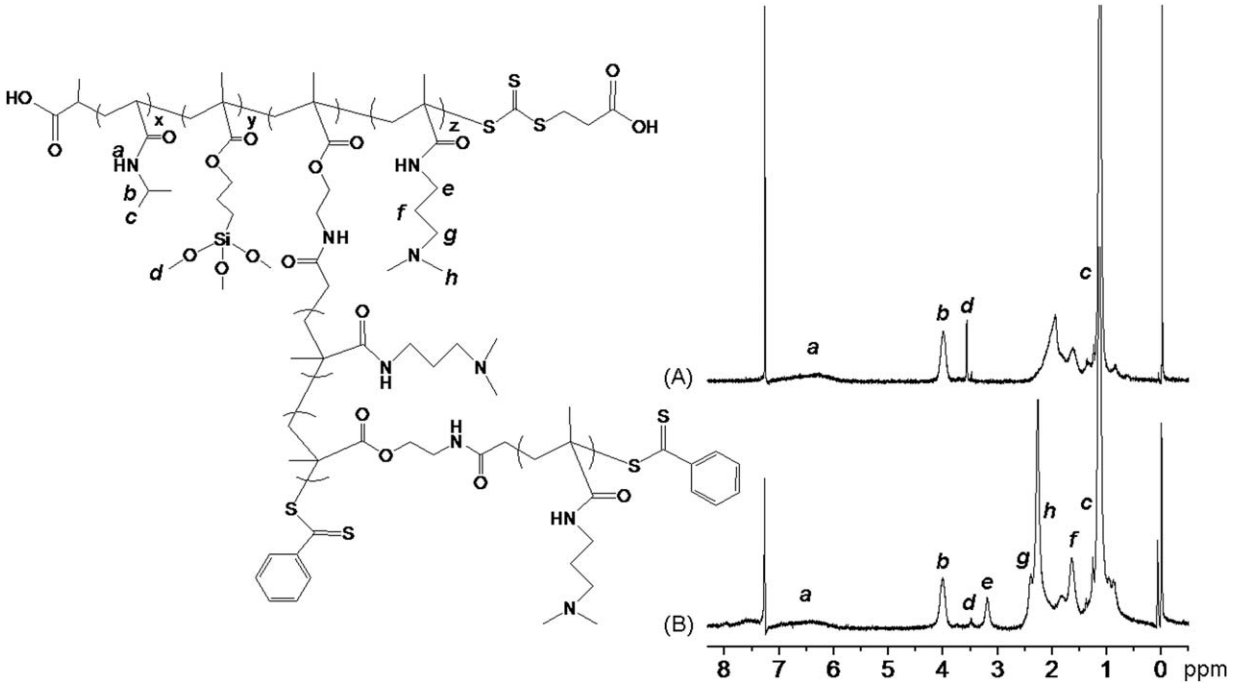

Figure 1. ^{1}H-NMR spectra of (A) P(NIPAAm$_{188}$-*co*-MPMA$_4$) and (B) branched P(NIPAAm$_{188}$-*co*-MPMA$_4$)-*b*-P(DMAPMAm$_{92}$) in $CDCl_3$.

$$\text{Cell viability } (\%) = [OD_{570(\text{samples})}/OD_{570(\text{control})} \times 100$$

where OD is optical density, $OD_{570(\text{control})}$ was obtained in the absence of micelles and $OD_{570(\text{samples})}$ was obtained in the presence of micelles.

RESULTS AND DISCUSSION

Synthesis of the Branched P(NIPAAm-*co*-MPMA)-*b*-PDMAPMAm Copolymer

The branched P(NIPAAm-*co*-MPMA)-*b*-PDMAPMAm diblock copolymer was synthesized by a two-step procedure, that is, the generation of the P(NIPAAm-*co*-MPMA) copolymer by RAFT polymerization with CPA as a chain-transfer agent (CTA), followed by synthesis of the branched P(NIPAAm-*co*-MPMA)-*b*-PDMAPMAm diblock copolymer via the RAFT polymerization of DMAEMA with P(NIPAAm-*co*-MPMA) as a macro-CTA and PAEM as a copolymerization monomer via the vinyl group and simultaneously as a CTA through the dithobenzoate moiety. The detailed synthesis route is illustrated in Scheme 1.

^{1}H-NMR was used to characterize the branched structure of the resulting diblock copolymers. Figure 1(A) shows the characteristic peaks of P(NIPAAm-*co*-MPMA). ^{1}H-NMR [$CDCl_3$, ppm, tetramethylsilane (TMS)]: 5.9–7.0 (a, —N*H*— in NIPAAm units), 4.0 [b, —C*H*$(CH_3)_2$ in NIPAAm units], 3.6 [d, —(OC*H*$_3$)$_3$ in MPMA units], 1.0 ppm [c, —CH(C*H*$_3$)$_2$ in NIPAAm units].

With respect to the integrity ratio of the block in the P(NIPAAm-*co*-MPMA) copolymer, the integrity ratio of peak b to peak d was 5.26:1; this indicated that the molar ratio of the two moieties was *n*(NIPAAm):*n*(MPMA) = 47:1 (where *n* is the number of monomer unit). Figure 1(B) shows the coexistence of the characteristic peaks of the P(NIPAAm-*co*-MPMA) and PDMAPMAm blocks. Upon comparison of Figure 1(A) to 2(B), new resonance signals were recorded at 3.2 ppm (e, —NHC*H*$_2$CH$_2$— in DMAPMAm units), 2.4 ppm [g, —CH$_2$C*H*$_2$N(CH$_3$)$_2$ in DMAPMAm units], 2.2 ppm [h, —CH$_2$CH$_2$N(C*H*$_3$)$_2$ in DMAPMAm units], and 1.6 ppm (f, —NHCH$_2$C*H*$_2$CH$_2$— in DMAPMAm units). All of the characteristic signals assigned to the block copolymer were clearly observed; this confirmed the successful synthesis of the target dicopolymer. The molar ratio of the MPMA and DMAPMAm units in P(NIPAAm-*co*-MPMA)-*b*-PDMAPMAm was calculated to be 1:21 from the integrity ratio (1:4.63) of the corresponding peaks (d and e). The characteristic peaks of the

Table I. Molecular Weights of the P(NIPAAm-*co*-MPMA) and P(NIPAAm-*co*-MPMA)-*b*-PDMAPMAm Copolymers as Measured by SEC–MALLS

Copolymer	M_n	M_w	M_n/M_w (PDI)	*dn*/*dc*
P(NIPAAm-co-MPMA)	14,700	20,400	1.38	0.092
P(NIPAAm-co-MPMA)-b-PDMAPMAm	22,900	36,100	1.57	0.092

PDI, polydispersity index.

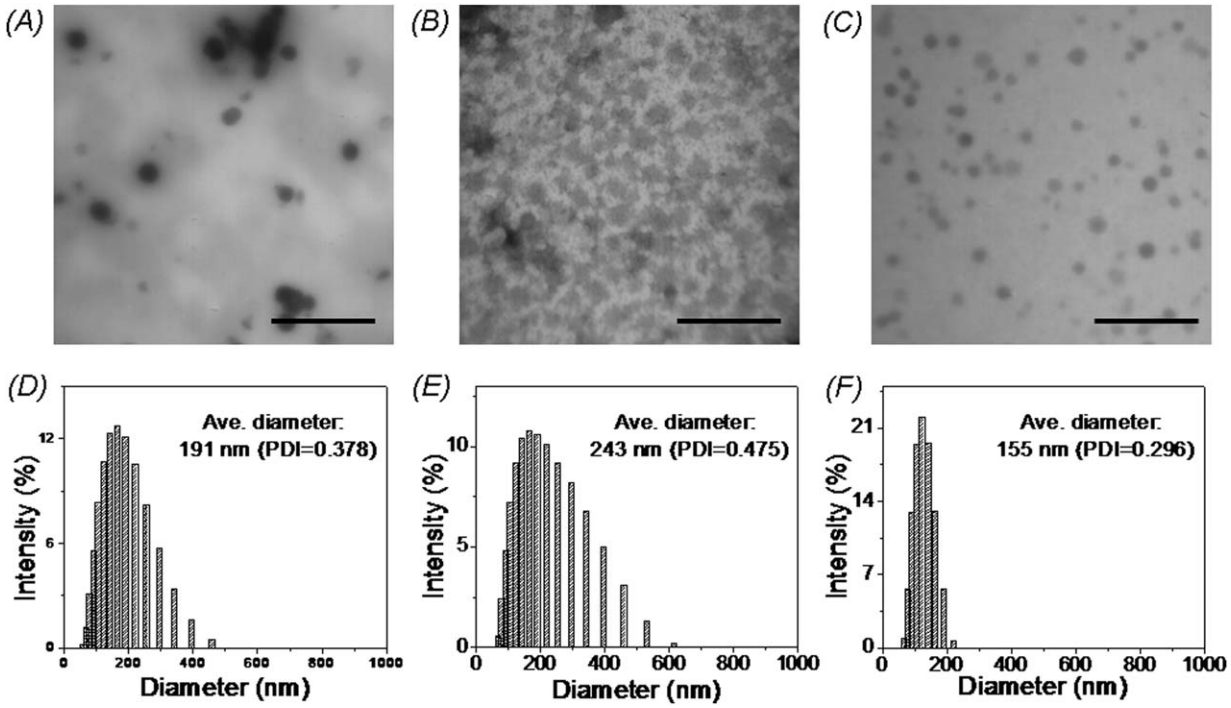

Figure 2. TEM micropictures and size distribution of CCL micelles in (A,D) DMF, (B,E) distilled water at 20°C, and (C,F) distilled water at 45°C. The scale bar is 700 nm.

P(NIPAAm-*co*-MPMA) polymer and PDMAPMAm polymer were attributed according to our previously published article.[39–41]

SEC–MALLS analyses were used to determine the molecular weights of the as-prepared polymers. As shown in Table I, the number-average molecular weight (M_w) and polydispersity [M_w/ number-average molecular weight (M_n)] of P(NIPAAm-*co*-MPMA)-*b*-PDMAPMAm (36,100 and 1.57) were both larger than that of P(NIPAAm-*co*-MPMA) (20,400 and 1.38). In addition, both polymers displayed unimodal elution traces (data not shown). These results also suggest the high reactivity of P(NIPAAm-*co*-MPMA) macro-CTA; therefore, the PAEM and DMAEMA monomers were both inserted efficiently into the macro-CTA; this led to an obvious increase in M_w of the final product by a further RAFT polymerization. Similarly, RAFT polymerization as a powerful tool for inserting the second or third block has also been reported in the literature.[42,43]

The molar ratio of the NIPAAm unit, MPMA unit, and DMAPMAm unit was 47:1:21 resulted from the integrity ratio of peaks b, d, and e was 5.26:1:4.63 from the ^{1}H-NMR spectrum when peak d was chosen to be the standard peak. The degrees of polymerization of the NIPAAm and MPMA units were calculated to be 188 and 4, respectively, on the basis of the molar ratio (47:1) obtained from the ^{1}H-NMR spectrum and the molecular weight of the P(NIPAAm-*co*-MPMA) block (20,400). The degree of polymerization of the DMAPMAm units was determined to be 92 on the basis of the molecular weight of the PDMAPMAm block (15,700). Such calculation based on the molecular weight results agreed well with the structure determined from ^{1}H-NMR. The resulting copolymer was thus denoted P(NIPAAm$_{188}$-*co*-MPMA$_4$)-*b*-P(DMAPMAm$_{92}$).

CCL Micelle Formation

3-(Trimethoxysilyl)propyl methacrylate (MPMA) is a commonly used inorganic crosslinking agent. It can facilely form a crosslinked structure by silica–silica bonds after an acid- or base-catalyzed sol–gel process. The small quantity of silica-based crosslinking in the polymer could stabilize the micellar structure with little effect on the characteristics of the copolymer. Furthermore, this crosslinking strategy has some virtues, such as its low cost, low toxicity, and easy purification, and is particularly applied in biomedical materials.[39,40,44] The morphology of the CCL micelles was observed by TEM. The lyophilized CCL micelles were redispersed in DMF to detect whether the crosslinking was successful. The typical photographs and size distributions are presented in Figure 2. As shown in Figure 2(A), the CCL micelles displayed a well-defined spherical shape with a mean size around 200 nm. Because the copolymer could be completely dissolved in DMF, the observed nanospheres indicated the preservation of the micelle structure due to the successful crosslinking of the micellar core. From the dynamic light scattering (DLS) data, the average size of the CCL micelles was 191 nm [Figure 2(D)]. The size difference was mainly attributed to the fact that the size measured by the DLS was swollen micelles in solution, and the size observed by TEM was dried micelles. A similar difference in size as a result of different measurement techniques was reported previously as well.[45,46] A schematic illustration of the self-assembly behavior of amphiphilic copolymers in an aqueous medium, the formation of CCL micelles and subsequent DL, and condensation with pDNA is presented in Figure 3.

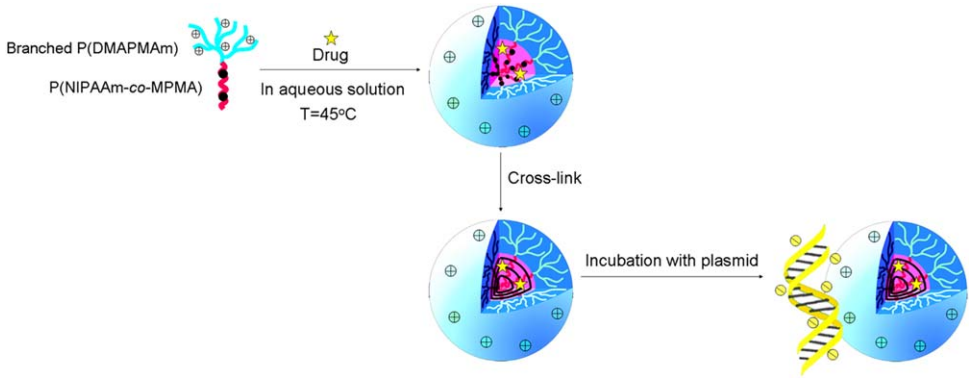

Figure 3. Schematic illustration of the micellization, crosslinking, and binding with DNA of the P(NIPAAm-*co*-MPMA)-*b*-PDMAPMAm aqueous solution (T = temperature). [Color figure can be viewed in the online issue, which is available at wileyonlinelibrary.com.]

Thermoresponsive Properties of the CCL Micelles

To determine whether these P(NIPAAm-*co*-MPMA)-*b*-PDMAPMAm micelles exhibited a thermal response, we measured the turbidity of the CCL micelle solutions as a function of the temperature. As shown in Figure 4, the LCST of the CCL micelles were determined to be about 38.0°C; this was higher than that of the pure PNIPAAm homopolymer. According to our previous study, the existence of terminal carboxylic acid groups affected the LCST, and such an effect was nonnegligible.[47] Thus, the elevated LCST was tentatively attributed to the end-group effect.

We further monitored the thermally induced structural changes in the P(NIPAAm-*co*-MPMA)-*b*-PDMAPMAm copolymer in water by ^{1}H-NMR analyses at different temperatures of 20 and 45°C, respectively, with D_2O as a solvent. The characteristic signals of both NIPAAm (peaks b and c) and DMAPMAm units (peaks e, g, h, and f) were distinct at 20°C (Figure 5). After transfer to an environment at 45°C, the characteristic peaks assigned to the NIPAAm units were significantly suppressed, whereas the peaks from the DMAPMAm units remained clearly visible; this indicated the phase transition of the PNIPAAm chains from the hydrophilic to the hydrophobic state.

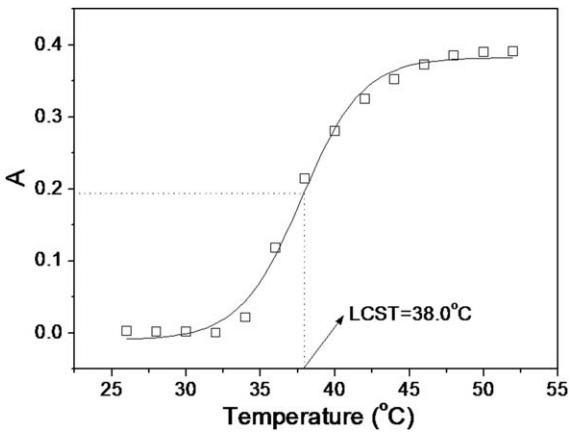

Figure 4. Turbidity of aqueous solutions of the CCL micelles in aqueous water. A = turbidity of aqueous solution of CCL micelles.

Thermally induced structural transformation of the crosslinked micelles was further visualized directly by TEM. Figure 2(B,C) show microphotographs of CCL micelles observed in a 20 and 45°C aqueous solution, respectively. The sizes of the CCL micelles were determined to be in the range 94–170 nm at 20°C and 56–113 nm at 45°C; this indicated the decrease of micelle size when the temperature increased from 20 to 45°C. The size change was due to the shrinkage and aggregation of the hydrophobic P(NIPAAm-*co*-MPMA) block at temperatures above its LCST; this led to a dehydrated micellar core domain with a compacted structure and decreased dimensions. Such a change against was also confirmed by the size variation of the micelle nanoparticles at different temperatures as determined by DLS; namely, the average sizes of the CCL micelles were 243 and 155 nm at 20 and 45°C, respectively [Figure 2(E,F)].

In Vitro Thermoresponsive Drug Release

To investigate the temperature-responsive drug-release profile of the CCL micelles, an antitumor drug, DOX, was encapsulated into the micelle core as a model drug. The DOX-loaded CCL micelles were prepared by dialysis at 40°C. EE and DL were determined to be 40.9 and 4.1%, respectively.

As shown in Figure 6, drug release at 40°C exhibited a faster cumulative release behavior than that recorded at 20°C. On the basis of the experiments, the cumulative drug-release values within 120 h at 20 and 40°C were 51.8 and 93.1%, respectively. The different drug-release behaviors were feasibly attributed to the structural changes in the CCL micelles at different temperatures. In the 40°C releasing medium, the shell of the branched PDMAPMAm was hydrophilic, whereas the core of the P(NIPAAm-*co*-MPMA) was hydrophobic. The drug diffused out from micelle core to the release medium primarily because of the concentration difference between the inside and the outside of the micelle. On the other hand, the swelling of the micellar core in place of the complete deformation of the micelle structure took place at 20°C because of the hydrophobic-to-hydrophilic transformation of the P(NIPAAm-*co*-MPMA) block and the effective crosslinking of the micellar structure. Cheng *et al.*[48] reported that the drug diffused out quickly for the deformation of noncrosslinked micelles under similar conditions. However, the swelling of the CCL micelles at low

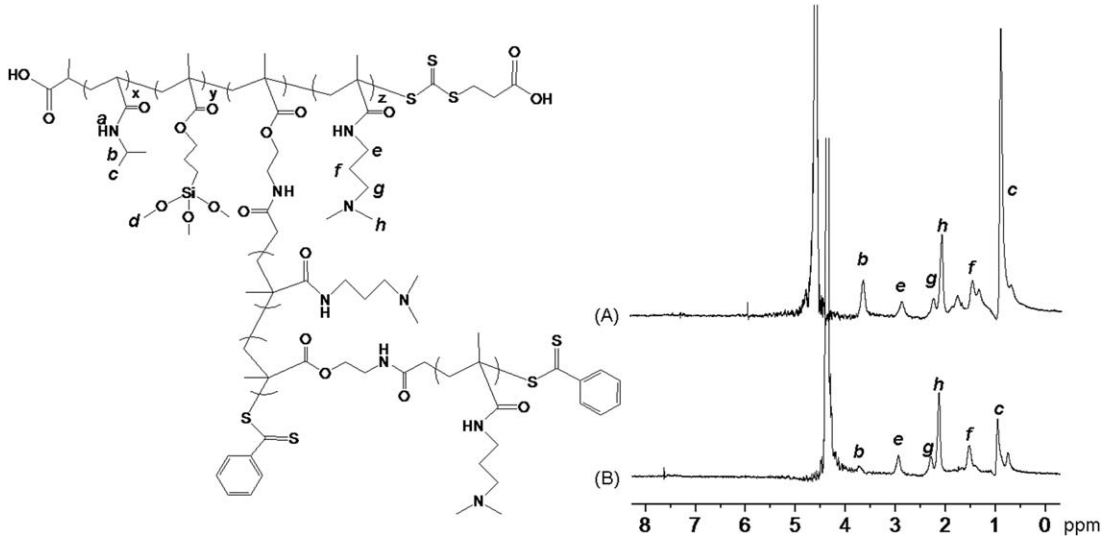

Figure 5. ^{1}H-NMR spectra of the CCL micelles in D_2O: (A) 20 and (B) 45°C.

temperatures in this study increased the diameter of the micelles; this prolonged the channel of drug diffusion and decreased the drug diffusion rate. This result was consistent with the reported literature.[40]

Here, a new branched double-hydrophilic block copolymer of P(NIPAAm-*co*-MPMA)-*b*-PDMAPMAm with thermal sensitivity was designed and synthesized. The core–shell micelle with the PNIPAAm moiety constructing the micellar core and the PDMAEMA moiety building the micellar shell could be facilely obtained by simple heating of the aqueous polymer solution to the temperature above the LCST of the PNIPAAm block. Therefore, in contrast to the classical dialysis method, such double-hydrophilic block-copolymer-based micelles could be prepared without the involvement of organic solvents. This method was environmentally friendly and suitable for the preparation of biomedical materials.[48–50] Furthermore, a slower and sustained-release profile of micelles was recorded at a temperature under its LCST; this indicated that it had potentially sustained release preparation at human body temperature.

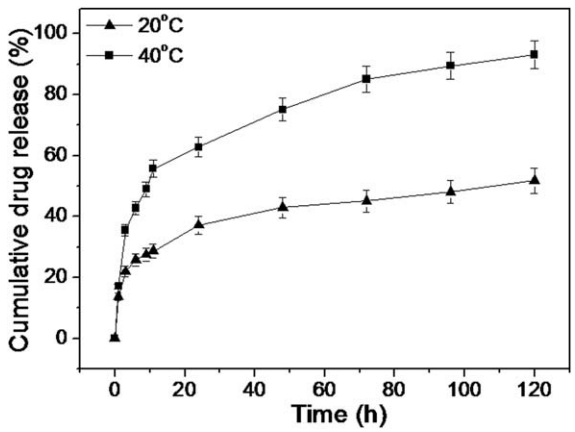

Figure 6. Cumulative drug release of the thermosensitive CCL micelles in PBS solution (pH 6.8) at different temperatures (20 and 40°C).

Gel Retardation Assay

Polycations can efficiently condense pDNA to form a so-called *polyplex,* which can protect pDNA against digestion by enzymes and package it into a compact unit. The resulting complex can facilitate endosomal escape because of a proton sponge effect and then realize unpackaging and the subsequent accumulation of pDNA in the nucleus of the target cells for gene transfection.[51] Agarose gel electrophoresis was carried out to evaluate DNA binding ability of the CCL micelles. As shown in Figure 7, the complete retardation of DNA immigration was recorded at an nitrogen/phosphor (N/P) ratio higher than 10, which confirmed the successful condensation of pDNA with CCL micelle formulation (Figure 7).

In Vitro Transfection

The transfection efficiency mediated by the CCL micelles was assessed in the 293T and HeLa cell lines, respectively, with luciferase as a reporter gene and branched polyethylenimine (bPEI; 25 kDa) at its optimal N/P ratio of 10 as a control. The efficiency of the CCL micelle/DNA complexes was evaluated at weight ratios from 5 to 30 w/w. The transfection efficiency of genetic vectors in serum-containing media can serve as a fundamental predictive model for their *in vivo* efficiency evaluation, so the *in vitro* transfection was investigated in both serum-free and 10% serum-containing media; this is a typical serum concentration for most *in vitro* biological assays.[52,53]

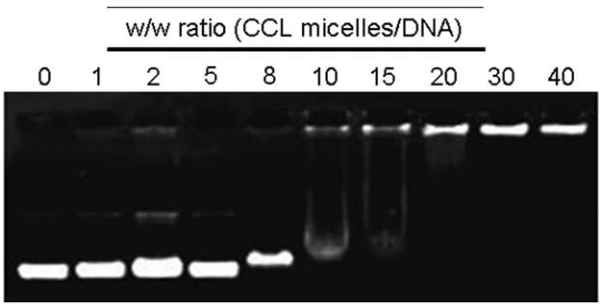

Figure 7. Agarose gel electrophoresis retardation assay of the CCL micelle/DNA complexes at weight ratios ranging from 0 to 40 w/w.

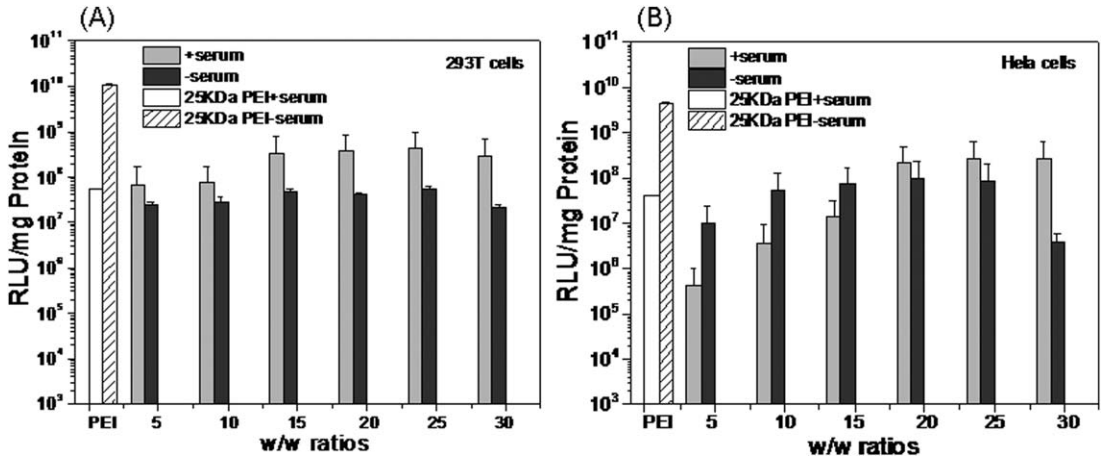

Figure 8. Transfection efficiency of the CCL micelle/DNA complexes at weight ratios ranging from 5 to 30 w/w in (A) 293T and (B) HeLa cells. The data are shown as mean plus or minus standard deviation ($n = 3$). $^*p < 0.05$ as compared with the data of bPEI. RLU = relative luciferase activity.

As shown in Figure 8, the transfection efficiency of the CCL micelle/DNA complexes at various N/P ratios in the absence of serum was lower than that of bPEI in both cell lines, but notably, the CCL micelles mediated comparable or even higher transfection efficiencies, especially in 293T cells, than bPEI in the presence of serum. The transfection efficiency of bPEI decreased significantly in the presence of serum; however, complexes formed by the CCL micelles exhibited a higher transfection activity in serum-containing media; this was likely due to the enhanced stability of the crosslinked micelle structure (Figure 8).

Antitumor Effect of the Drug- and p53-Loaded CCL Micelles

Codelivery of an antitumor drug and gene by one vehicle could reduce the frequency of administration, improve patient compliance, and achieve a synergistic therapeutic effect. To validate whether the antitumor effect of codelivery was better than single chemotherapy, an MTT assay was performed to evaluate the *in vitro* cytotoxicity of the pure CCL micelles, DOX-loaded CCL micelles, and DOX- and p53-loaded CCL micelles. As shown in Figure 9, the cytotoxicity for all three systems increased with increasing concentration. The cell viability was reported to be below 30% when the concentration of bPEI was 0.05 mg/L;[11,54,55] however, the cell viability was still 81.5% when the concentration of the pure CCL micelles was 0.8 mg/L. Obviously, the toxicity of the pure CCL micelles was much lower than that of bPEI. Compared to the insignificant cytotoxicity of the pure CCL micelles, the cytotoxicity of the other two formulations increased dramatically, especially for the DOX- and p53-loaded CCL micelles. The cell viability was 55.1% when the concentration of the DOX-loaded CCL micelles was 0.8 mg/L, and the viability further decreased to 40.6% for the DOX- and p53-loaded CCL micelles at the same concentration. The results confirm that p53 sensitized the tumor cells to DOX;[2] this would lead to a more potent antitumor efficacy. On the basis of these results, an efficient anticancer formulation based on DOX- and p53-loaded CCL micelles was developed successfully as expected. Because the *in vitro* drug release could not simulate the cell experiments completely for the complexity of intracellular environment, the results of the two experiments did not absolutely match.

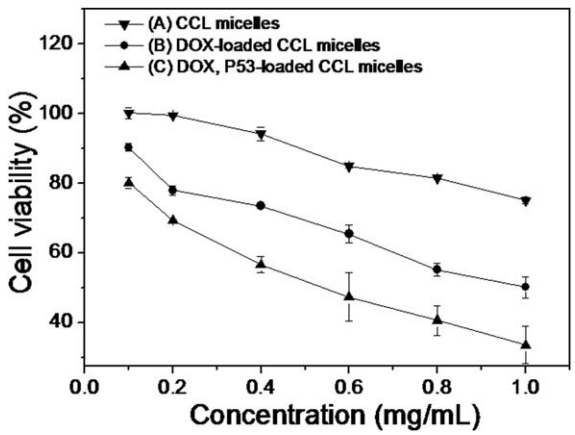

Figure 9. Viability of the HeLa cells after they were incubated with blank CCL micelles, DOX-loaded CCL micelles, and DOX, P53-loaded CCL micelles for 4 h at concentrations ranging from 0.1 to 1.0 mg/mL.

CONCLUSIONS

In summary, a thermoresponsive P(NIPAAm-*co*-MPMA)-*b*-PDMAPMAm copolymer with a branched architecture was designed and synthesized by successive RAFT polymerizations. CCL micelles composed of a hydrophobic P(NIPAAm-*co*-MPMA) core for DL and a cationic PDMAPMAm shell for DNA condensation were fabricated with this copolymer. The resulting CCL micelles mediated a higher transfection efficacy in serum-containing media than the golden standard for transfetcion, bPEI. More importantly, the synergistic therapeutic effect resulting from the codelivery of p53 and DOX with this CCL micelle formulation was much better than that from sole chemotherapy and demonstrated great potential for integrated drug and gene therapy.

ACKNOWLEDGMENTS

The authors are grateful for the financial support from the China Postdoctoral Science Foundation (contract grant number 2012M511597).

REFERENCES

1. Wu, D. Q.; Li, Z. Y.; Li, C.; Fan, J. J.; Lv, B.; Chang, C.; Cheng, S. X.; Zhang, X. Z.; Zhuo, R. X. *Pharm. Res.* **2009**, *27*, 187.
2. Wiradharma, N.; Tong, Y. W.; Yang, Y. Y. *Biomaterials* **2009**, *30*, 3100.
3. Ma, M.; Yuan, Z. F.; Chen, X. J.; Li, F.; Zhuo, R. X. *Acta Biomater.* **2012**, *8*, 599.
4. Aagaard, L.; Rossi, J. *J. Drug Delivery Rev.* **2007**, *59*, 75.
5. Cao, N.; Cheng, D.; Zou, S.; Ai, H.; Gao, J.; Shuai, X. *Biomaterials* **2011**, *32*, 2222.
6. Shapira, A.; Livney, Y. D.; Broxterman, H. J.; Assaraf, Y. G. *Drug Resist. Update* **2011**, *14*, 150.
7. Zhu, C.; Jung, S.; Luo, S.; Meng, F.; Zhu, X.; Park, T. G.; Zhong, Z. *Biomaterials* **2010**, *31*, 2408.
8. Cheng, D.; Cao, N.; Chen, J.; Yu, X.; Shuai, X. *Biomaterials* **2012**, *33*, 1170.
9. Wang, Y.; Gao, S.; Ye, W. H.; Yoon, H. S.; Yang, Y. Y. *Nat. Mater.* **2006**, *5*, 791.
10. Shi, S.; Zhu, X.; Guo, Q. F.; Wang, Y.; Zuo, T.; Luo, F.; Qian, Z. *Int. J. Nanomed.* **2012**, *7*, 1749.
11. Han, K.; Chen, S.; Chen, W. H.; Lei, Q.; Liu, Y.; Zhuo, R. X.; Zhang, X. Z. *Biomaterials* **2013**, *34*, 4680.
12. Nam, K.; Nam, H. Y.; Kim, P. H.; Kim, S. W. *Biomaterials* **2012**, *33*, 8122.
13. Lambert, B.; Charreyre, M. T.; Chaix, C.; Pichot, C. *Polymer* **2007**, *48*, 437.
14. Wei, H.; Volpatti, L. R.; Sellers, D. L.; Maris, D. O.; Andrews, I. W.; Hemphill, A. S.; Chan, L. W.; Chu, D. S.; Horner, P. J.; Pun, S. H. *Angew. Chem. Int. Ed.* **2013**, *52*, 1.
15. Lowe, A. B.; McCormick, C. L. *Prog. Polym. Sci.* **2007**, *32*, 283.
16. De, P.; Li, M.; Gondi, S.; Sumerlin, B. S. *J. Am. Chem. Soc.* **2008**, *130*, 11288.
17. Chang, C.; Wei, H.; Wu, D. Q.; Yang, B.; Chen, N.; Cheng, S. X.; Zhang, X. Z.; Zhuo, R. X. *Int. J. Pharm.* **2011**, *420*, 333.
18. Xu, J.; Tao, L.; Liu, J.; Bulmus, V.; Davis, T. P. *Macromolecules* **2009**, *42*, 6893.
19. Lin, Y.; Liu, X.; Li, X.; Zhan, J.; Li, Y. *J. Polym. Sci. Part A: Polym. Chem.* **2006**, *45*, 26.
20. Li, Y. T.; Armes, S. P. *Macromolecules* **2009**, *42*, 939.
21. Vogt, A. P.; Sumerlin, B. S. *Macromolecules* **2008**, *41*, 7368.
22. Thurecht, K. J.; Blakey, I.; Peng, H.; Squires, O.; Hsu, S.; Alexander, C.; Whittaker, A. K. *J. Am. Chem. Soc.* **2010**, *132*, 5336.
23. Jikei, M.; Kakimoto, M. *Prog. Polym. Sci.* **2001**, *26*, 1233.
24. Voit, B. *J. Polym. Sci. Part A: Polym. Chem.* **2000**, *38*, 2505.
25. Mintzer, M. A.; Simanek, E. E. *Chem. Rev.* **2009**, *109*, 259.
26. Wolff, J. A.; Rozema, D. B. *Mol. Ther.* **2008**, *16*, 8.
27. Wang, R.; Zhou, L.; Zhou, Y.; Li, G.; Zhu, X.; Gu, H.; Jiang, X.; Li, H.; Wu, J.; He, L.; Guo, X.; Zhu, B.; Yan, D. *Biomacromolecules* **2010**, *11*, 489.
28. Martello, F.; Piest, M.; Engbersen, J. F.; Ferruti, P. *J. Controlled Release* **2012**, *164*, 372.
29. Momparler, R. L.; Karon, M.; Siegel, S. E.; Avila, F. *Cancer Res.* **1976**, *36*, 2891.
30. Hortobagyi, G. N. *Drugs* **1997**, *54*, 1.
31. Lee, T. K.; Lau, T. C.; Ng, I. O. *Cancer Chemother. Pharmacol.* **2002**, *49*, 78.
32. Shen, Y.; White, E. *Adv. Cancer Res.* **2001**, *82*, 55.
33. Xu, L.; Pirollo, K. F.; Chang, E. H. *J. Controlled Release* **2001**, *74*, 115.
34. Lu, X.; Wang, Q. Q.; Xu, F. J.; Tang, G. P.; Yang, W. T. *Biomaterials* **2011**, *32*, 4849.
35. Wetering, P.; Moret, E. E.; Sehuurmans-Nieuwenbroek, N. M.; Steenbergen, M. J.; Hennink, W. E. *Bioconjug. Chem.* **1999**, *10*, 589.
36. Chang, C.; Wei, H.; Feng, J.; Wang, Z. C.; Wu, X. J.; Wu, D. Q.; Cheng, S. X.; Zhang, X. Z.; Zhuo, R. X. *Macromolecules* **2009**, *42*, 4838.
37. Zarzhitsky, S.; Rapaport, H. *J. Colloid Interface Sci.* **2011**, *360*, 525.
38. Zhou, Q.; Zhang, Z.; Chen, T.; Guo, X.; Zhou, S. *Colloid Surf. B* **2011**, *86*, 45.
39. Wei, H.; Cheng, C.; Chang, C.; Chen, W. Q.; Cheng, S. X.; Zhang, X. Z.; Zhou, R. X. *Langmuir* **2008**, *24*, 4564.
40. Chang, C.; Wei, H.; Feng, J.; Wang, Z. C.; Wu, X. J.; Wu, D. Q.; Cheng, S. X.; Zhang, X. Z.; Zhuo, R. X. *Macromolecules* **2009**, *42*, 4838.
41. Zhu, J. L.; Cheng, H.; Jin, Y.; Cheng, S. X.; Zhang, X. Z.; Zhuo, R. X. *J. Mater. Chem.* **2008**, *18*, 4433.
42. Convertine, A. J.; Lokitz, B. S.; Vasileva, Y.; Myrick, L. J.; Scales, C. W.; Lowe, A. B.; McCormick, C. L. *Macromolecules* **2006**, *39*, 1724.
43. Madsen, J.; Armes, S. P.; Bertal, K.; Lomas, H. *Biomacromolecules* **2008**, *9*, 2265.
44. Zhang, Y. F.; Luo, S. Z.; Liu, S. Y. *Macromolecules* **2005**, *38*, 9813.
45. Morita, T.; Horikiri, Y.; Suzuki, T.; Yoshino, H. *Int. J. Pharm.* **2001**, *219*, 127.
46. Giacomelli, C.; Schmidt, V.; Borsali, R. *Macromolecules* **2007**, *40*, 2148.
47. Chang, C.; Wei, H.; Quan, C. Y.; Li, Y. Y.; Liu, J.; Wang, Z. C.; Cheng, S. X.; Zhang, X. Z.; Zhuo, R. X. *J. Polym. Sci. Part A: Polym. Chem.* **2008**, *46*, 3048.
48. Cheng, C.; Wei, H.; Shi, B. X.; Cheng, H. *Biomaterials* **2008**, *29*, 497.
49. Zhou, Y.; Jiang, K.; Song, Q.; Liu, S. *Langmuir* **2007**, *23*, 13076.
50. Zhang, X.; Li, J.; Li, W.; Zhang, A. *Biomacromolecules* **2007**, *8*, 3557.
51. Behr, J. P. *Chimia* **1997**, *51*, 34.
52. Kleemann, E.; Neu, M.; Jekel, N.; Fink, L.; Schmehl, T.; Gessler, T.; Seeger, W.; Kissel, T. *J. Controlled Release* **2005**, *109*, 299.
53. Luo, X.; Huang, F.; Qin, S.; Wang, H.; Feng, J.; Zhang, X.; Zhuo, R. *Biomaterials* **2011**, *32*, 9925.
54. Cheng, H.; Zhu, J. L.; Sun, Y. X.; Cheng, S. X.; Zhang, X. Z.; Zhuo, R. X. *Bioconjug. Chem.* **2008**, *19*, 1368.
55. Wang, H. Y.; Chen, J. X.; Sun, Y. X.; Deng, J. Z.; Li, C.; Zhang, X. Z.; Zhuo, R. X. *J. Controlled Release* **2011**, *155*, 26.